Thorac Res Pract. 2026;27(1):57-67 **DOI:** 10.4274/ThoracResPract.2025.2025-6-2

Review

Artificial Intelligence in Pleural Diseases: Current Applications and Next Steps

Ferhan Karataş[1], Öner Dikensoy[1,2]

[1]Department of Pulmonary Diseases, Koç University Hospital, İstanbul, Türkiye
[2]Department of Pulmonary Diseases, Koç University Faculty of Medicine, İstanbul, Türkiye

Cite this article as: Karataş F, Dikensoy Ö. Artificial intelligence in pleural diseases: current applications and next steps. *Thorac Res Pract.* 2026;27(1):57-67

ABSTRACT

Pleural diseases pose a significant burden on healthcare systems due to diagnostic challenges and high costs. Artificial intelligence (AI) has the potential to provide faster, more accurate, and more reliable results in the diagnosis of these diseases. This review evaluates the current status of AI technologies in the diagnosis of pleural effusion (PE), malignant PE, tuberculosis pleurisy (TP), pneumothorax, and malignant pleural mesothelioma (MPM). Deep learning algorithms developed for radiological diagnosis provide high sensitivity and specificity in determining the presence and severity of PE. AI models that integrate clinical parameters such as chest computed tomography (CT), positron emission tomography (PET)-CT, and tumour markers in distinguishing between benign and malignant effusions have significantly improved diagnostic accuracy (area under the curve: >0.90). In cytological diagnosis, computer-assisted systems such as Aitrox have demonstrated performance comparable to that of expert cytopathologists in diagnosing malignant effusions. In the diagnosis of TP, AI models outperform conventional diagnostic methods, particularly when combined with laboratory parameters such as adenosine deaminase. Food and Drug Administration-approved AI models are effectively used for the rapid diagnosis of pneumothorax and for emergency interventions. In MPM diagnosis, AI models using PET-CT images and three-dimensional segmentation offer significant advantages in prognostic evaluation and treatment response monitoring. However, large-scale, multi-centre studies are needed to standardise and generalise AI models. In light of these developments, AI may fundamentally change the diagnostic management of pleural diseases.

KEYWORDS: Artificial intelligence, diagnostic methods, mesothelioma, pleural diseases, pneumothorax, tuberculosis

Received: 18.06.2025 ***Revision Requested:*** 03.09.2025 ***Last Revision Received:*** 09.09.2025

Accepted: 24.09.2025 ***Epub:*** 15.01.2026 ***Publication Date:*** 30.01.2026

INTRODUCTION

Pleural diseases are heterogeneous, with diverse etiologies posing complex diagnostic and therapeutic challenges.[1,2] Pleural diseases constitute a serious burden on healthcare systems and patients. They represent a significant burden, with an estimated annual incidence of 1.5 million cases in the USA and hospitalization costs exceeding 10 billion dollars.[1-4] Despite established diagnostic principles, no single method adequately meets clinical needs, underscoring the demand for faster and more accurate tools.[2,3]

Artificial intelligence (AI), defined as the simulation of human cognition through machine learning (ML), deep learning (DL), and data analysis, has recently become an essential component of healthcare.[5-7] Advances in big data and computational power have enabled AI to provide rapid, precise, and reliable analysis of radiological and clinical data, improving diagnostic accuracy and reducing clinician workload.[3,5-7] While initially developed for imaging, AI in respiratory medicine is now applied not only to lung cancer screening but also to pleural effusion (PE) and pneumothorax, and has demonstrated high diagnostic performance in these applications. Well-trained AI systems integrating clinical, radiological, and laboratory data support physicians with greater accuracy and reduced need for immediate specialist access. Consequently, AI is expected to play an increasingly important role in chest medicine.[3,5,6] A systematic review confirmed that AI-assisted observers outperformed human readers in detecting thoracic pathologies

Corresponding author: Ferhan Karataş, MD, e-mail: fkaratas19@hotmail.com, fkaratas@kuh.ku.edu.tr

on chest X-rays (CXR) and computed tomography (CT) scans, achieving higher sensitivity, specificity, accuracy, and area under the curve (AUC).[8]

This review discusses the current status, potential advantages, and limitations of AI applications in the diagnosis of pleural diseases, and comprehensively evaluates the potential contributions of these technologies to future clinical applications inlight of the existing literature.

METHODS

A comprehensive search of the PubMed database was performed, without restriction on publication dates, using combinations of the following search terms: "pleural disease", "pleural effusion", "pneumothorax", "pleural mesothelioma", "tuberculous pleurisy", "artificial intelligence", "machine learning", "deep learning", "ultrasound", "cytology", and "PET-CT". We included English-language human studies that reported the development, validation, or clinical impact of AI systems in pleural diseases across imaging [CXR, chest CT, positron emission tomography (PET)-CT, lung ultrasound], cytology/whole-slide imaging (WSI), and laboratory/biomarker data. We excluded non-pleural AI studies, editorials, letters without primary data, and purely technical papers lacking clinical outcomes. Reference lists and recent reviews were screened to identify additional relevant publications.

Technique and Modality Overview

Various imaging and laboratory modalities have been used in AI applications for pleural diseases. CXR is mainly used for triage of conditions such as pneumothorax and gross effusion. Chest CT allows detailed segmentation and complexity scoring of effusions. PET-CT provides additional differentiation between malignant and benign processes, as well as prognostic information in malignant pleural mesothelioma (MPM). Cytology with WSI supports benign-malignant triage in effusion samples. Lung ultrasound is increasingly being studied for real-time guidance and monitoring, though data remain preliminary. Figure 1 illustrates the overall workflow of AI applications in pleural diseases across different imaging and laboratory modalities, while Table 1 summarizes their main tasks, reported performance metrics, and current readiness levels.

Main Points

- Artificial intelligence (AI)-based imaging algorithms achieve high diagnostic performance in pleural diseases, with deep learning models on chest computed tomography (CT) and positron emission tomography-CT consistently reporting area under the curve values >0.90 for detecting pleural effusion (PE) and differentiating malignant from benign effusions.
- Automated segmentation and quantification tools improve reproducibility and workflow efficiency, particularly for PE volume assessment and malignant pleural mesothelioma follow-up, reaching near–expert-level agreement while reducing clinician workload.
- Multimodal AI models that integrate imaging with clinical and laboratory data outperform single-modality approaches, enhancing diagnostic accuracy in malignant PE and tuberculous pleurisy, often surpassing traditional biomarkers alone.
- AI-assisted cytology systems demonstrate diagnostic accuracy comparable to experienced cytopathologists, offering objective and rapid triage of malignant PEs and helping address inter-observer variability and workforce limitations.
- Despite promising results, most AI applications lack large-scale prospective validation, highlighting the need for multicenter studies, standardized protocols, and careful clinical integration before routine adoption in pleural disease management.

Artificial Intelligence in Radiological Diagnosis of Pleural Effusion

In a study, the AI model developed using 600 posterior-anterior chest radiographs had a sensitivity of 95%, a specificity of 97%, and an AUC of 97% for the detection of PE.[9] The same study also showed that abnormal radiological findings, such as air-fluid level, atelectasis, bleb, cardiomegaly, bone fracture, infiltration, mass, nodule, obstructive airway disease, pneumonia, and scoliosis, which may introduce bias, did not affect the algorithm's performance.

The AI model developed to assess PE severity may aid in treatment effectiveness and management. In a study evaluating the presence and severity of PE by AI in chest radiographs of chronic obstructive pulmonary disease patients, the model showed 85.4% accuracy (AUC: 0.95) for non-PE images; 12.5% of the 14.5% errors were mild PE.[10] Prediction accuracy rates for non-PE, small, moderate, and large effusions were 83.95%, 74.19%, 62.16%, and 50%, respectively. Zhou et al.[11] developed DL models to detect and segment cardiomegaly, pneumothorax, and PE on chest radiographs. A high-quality, labeled radiograph dataset was created, with lesion regions annotated by radiologists. The model used AP75 (overlap ≥75% between predicted and actual lesion regions) as the performance metric. High accuracy was achieved in detecting cardiomegaly (AP75: 98.0%), pneumothorax (AP75: 71.2%), and PE (AP75: 78.2%). Segmentation performance, evaluated using the dice similarity coefficient (DSC), was also strong (e.g., lung-field dice: 0.960). Detection and semi-quantitative analysis times with DL were significantly shorter than those of radiologists ($P < 0.001$), potentially expediting clinical workflows. These models show promise in automating lesion detection and quantitative analysis, supporting radiologists' diagnostic decision-making.

In a retrospective study, a series of DL-based sequential models was developed to automatically detect, segment, and classify PE as simple or complex using CT images from 2,659 patients.[12] A detection-segmentation network based on the self-configuring nnU-Net architecture achieved 99% sensitivity, 98% specificity, and a DSC of 0.89, matching human-level volumetric consistency.

Five classification models using the random forest (RF) algorithm, based on radiological features (hyperdense fluid, pleural thickening, gas, loculation) and radiomic features, reached an AUC of 0.77 for classifying simple vs. complex PE. Notably, pleural thickening yielded an AUC of 0.91, and hyperdense fluid achieved a negative predictive value (NPV) of

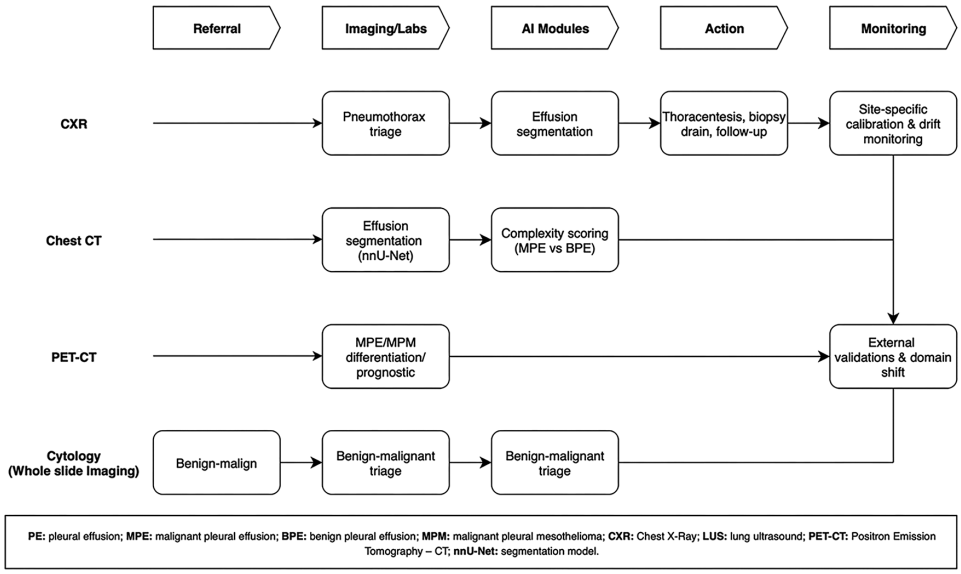

Figure 1. Workflow of artificial intelligence in pleural diseases by modality

Referral → imaging/labs (CXR, chest CT, PET-CT, LUS; cytology if present) → AI modules (triage, detection/segmentation, differential diagnosis, risk flags) → clinician review with thresholds → action (thoracentesis, biopsy, drain, follow-up) → monitoring (volume change, cytology triage)

Note: Performance pitfalls (e.g., small pneumothoraces on AP CXR and skin folds mimicking pneumothorax) highlight the need for site-specific calibration and continuous monitoring. In addition, all AI outputs are intended to function as decision-support tools and must be reviewed and validated by a physician before being used to guide clinical action

CXR: chest X-ray, CT: computed tomography, PET: positron emission tomography, LUS: lung ultrasound, AI: artificial intelligence, MPE: malignant pleural effusion, BPE: benign pleural effusion, MPM: malignant pleural mesothelioma, LUS: lung ultrasound, nnU-Net: segmentation model

Table 1. Overview of imaging and laboratory modalities used in artificial intelligence applications for pleural diseases

Modality	Main AI task(s)	Reported performance	Notes
CXR	Pneumothorax triage, effusion detection	Sensitivity 84-95%, specificity 88-97%, AUC ≈ 0.95	FDA-cleared tools available
Chest CT	Effusion segmentation, simple vs. complex PE classification	DSC 0.89; ICC ≥0.995	Highly reproducible, underestimates absolute volume
PET-CT	MPE vs. BPE differentiation, MPM prognosis	AUC up to 0.97	Small cohorts; potential in multimodal fusion
Cytology (WSI)	Malign vs. benign triage	AUC ≈ 0.95; accuracy >90%	Comparable to expert cytopathologists
LUS	Effusion detection/segmentation	Accuracy >90%, DSC 0.70	Operator dependence reduced with AI

Note: Reported performance values vary depending on dataset size, study design, and validation method. "Readiness" refers to current status: Research (tested in retrospective or single-center studies) vs. FDA-cleared/deployed (approved tools already used in clinical workflows)

AI: artificial intelligence, CXR: chest X-ray, CT: computed tomography, PET: positron emission tomography, WSI: whole-slide imaging, LUS: lung ultrasound, PE: pleural effusion, MPE: malignant pleural effusion, BPE: benign pleural effusion, MPM: malignant pleural mesothelioma, DSC: Dice similarity coefficient, ICC: intraclass correlation coefficient, AUC: area under the curve, FDA: Food and Drug Administration

0.94. Segmentation accuracy remained unaffected by contrast use or effusion complexity, confirming the model's robustness across diverse clinical scenarios.

In a prospective study of 79 patients, the accuracy of an AI algorithm that quantifies PE volume change via automatic segmentation of pre- and post-thoracentesis CT images was compared with actual drainage volumes.[13] The fully automated method underestimated drainage by 13.1%, while the semi-automated method, corrected by a thoracic radiologist, underestimated by 10.9% drainage, and the error increased linearly with fluid volume. Despite this, both agreement between methods [fully automated vs. semi-automated; intraclass correlation coefficient (ICC): 0.99] and test-retest reliability ICC: ≥0.995 were excellent. These results indicate that, although AI-based CT measurements are highly reproducible for clinical use, they consistently underestimate actual volumes, underscoring the need for calibration or correction, and highlighting the importance of accounting for algorithmic bias in quantitative monitoring of PE treatment response.

Artificial Intelligence in the Diagnosis of Malignant Pleural Effusion

The gold standard for differentiating malignant from benign PE is cytopathological examination of samples obtained by thoracentesis or pleural biopsy. Although they have high

specificity, their disadvantages include low positivity rates in pathological diagnosis, invasiveness, and high cost.[14,15] Therefore, non-invasive diagnostic methods with high sensitivity and improved diagnostic performance are needed.

Chest CT is one of the initial tools for the differential diagnosis of PE, and AI models may help reduce radiologists' workload. Wang et al.[16] developed an AI model that used chest CT features. The study analysed 918 PE cases—607 internal and 311 external—and created a training cohort of 362 cases from another centre. The model follows a two-stage structure: first, PE areas were segmented from CT images, producing masks with high overlap with expert-defined boundaries (mean DSC: 87.6%). Second, three dimensional (3D) PE masks and full CT volumes were used to classify the effusion as malignant or benign. The internal test cohort showed an AUC of 0.883, a sensitivity of 78.4%, and a specificity of 86.2%. In the external cohort, the AUC was 0.842, with 89.4% sensitivity and 65.1% specificity. Incorporating clinical data—such as sex, age, laterality, and PE volume—further improved AUCs in all three cohorts. The model detects suspicious areas, performs fine segmentation, and holistically analyzes chest CT features to differentiate benign pleural effusion (BPE) from MPE. The authors concluded that this AI model may assist radiologists and clinicians in PE case management.

Ozcelik et al.[17] compared the quantitative features of PE on CT scans with cytological results. The positive predictive value (PPV), NPV, sensitivity, specificity, and accuracy of the DL model for the diagnosis of MPE were reported as 93.3%, 86.67%, 87.5%, 92.86%, and 90%, respectively, for differentiating benign from malignant PE. In another study, the applicability of one DL model and five ML models in differentiating MPE from BPE was investigated.[18] In this study, a total of 898 patients were included; data from 726 patients were used for training and testing the models, and data from 172 patients were used for the prospective validation. The diagnostic performance, as measured by the AUC, was 90.9% in the training set, 88.3% in the test set, and 86.6% in the validation set. When laboratory findings were included, the addition of the carcinoembryonic antigen (CEA) level in PE showed the best diagnostic performance, with an AUC of 90.9%, a sensitivity of 82.09%, and a specificity of 91.37% at a cut-off value of 3.6 ng/mL. Clinically, this threshold can help non-invasively distinguish malignant from benign effusions and guide decisions about whether to proceed with or defer invasive procedures. The results of this study show that using AI to guide physicians in PE management is a highly effective, non-invasive diagnostic aid.

In another study, an ML model based on clinical, blood, and pleural-fluid examination features was developed to classify the etiology of PE into five groups, including transudate, malignant, parapneumonic, tuberculous pleurisy (TP), and others.[19] In this retrospective study, 18 basic features were identified by feature selection (FS), including history of malignancy; blood test results such as C-reactive protein and albumin; and pleural fluid characteristics such as lactate dehydrogenase (LDH), protein, adenosine deaminase (ADA), and CEA. The model's AUC for detecting MPE was 0.930 in the validation set and 0.916 in the extra validation set. The light gradient boosting machine (GBM) model showed the best performance, with accuracies of 81.8% and 78.7% in the validation and extra validation datasets, respectively. This ML algorithm provided high accuracy in the differential diagnosis of PE and may be useful as a clinical decision-support system by guiding clinicians regarding the necessity of invasive procedures.

Zhang et al.[20] developed five ML models—XGBoost, logistic regression (LR), Bayesian additive regression trees, RF, and support vector machine (SVM)—to assess the diagnostic performance of CEA, CA19-9, CA125, and CA15-3 in PE. Using these models, 319 PE cases were analyzed using both individual and combined tumor markers. Among single-marker models, the XGBoost model with CEA showed the highest AUC (0.895) and sensitivity (80%), while that with CA153 had the highest specificity (98%). Among marker combinations, the XGBoost model with CEA + CA153 achieved the highest AUC (0.921) and sensitivity (85%), whereas both the XGBoost model with CA125 + CA153 and the LR model with CEA + CA153 + CA19-9 achieved the highest specificity (97%). In another study, five AI models were developed using laboratory data from 2,352 patients.[21] The XGBoost model outperformed other models, with AUCs of 0.903, 0.918, and 0.886 in the training, validation, and test cohorts, respectively; it also achieved specificities of 89.2%, 93.4%, and 91.8%, and sensitivities of 86.1%, 84.4%, and 80.4%. PE CEA was the most important predictor, followed by serum CYFRA21-1, PE CA125, haematocrit, creatinine, calcium, and neutrophil percentage. The model also outperformed the standalone PE CEA in differentiating MPE from BPE.

The reported sensitivity of pleural fluid cytology is between 40% and 90%, depending on the tumor cell type.[22] However, inconsistencies are observed among pathologists in manual screening results, which suggest that these examinations are subjective. Although pleural metastasis indicates advanced-stage disease with a survival of 3-12 months, patients' life expectancy can be prolonged by prompt diagnosis. Early, accurate, rapid, and objective diagnoses can be achieved using automatic image analysis. Therefore, the development of computer-aided diagnosis (CAD) systems is essential. Win et al.[23] developed a CAD system for the diagnosis of MPE. In this system, 201 cellular features were analysed, and high diagnostic performance was achieved, with 87.9% sensitivity, 99.4% specificity, and 98.7% accuracy for the diagnosis of MPE. In another study, an AI model called "Aitrox" was applied to classify benign and malignant lung cancer cells in PE cytology.[24] The diagnostic performance of the model was compared between junior and senior cytopathologists. The "Aitrox" AI model featured in this study is a weakly supervised DL method based on a deep convolutional neural network (DCNN) designed to classify benign and malignant cases in lung cytological images at the WSI level. Aitrox AI achieved 91.67% accuracy, 87.5% sensitivity, and 94.4% specificity, with an AUC of 0.9526. These rates were higher than those of young cytopathologists and similar to those of senior cytopathologists. It has been demonstrated that this AI model provides more objective and consistent results than those of cytopathologists and may help alleviate the shortage of cytopathologists. Current research shows that AI can be used as an effective tool in the rapid cytological diagnosis of MPE. In addition to classifying PE as malignant or benign, AI

models could be developed to detect atypical cases or cases suspected of being malignant.

In a study using an AI algorithm to screen PET-CT scans for the diagnosis of PE in patients with malignancy, a sensitivity of 95.5%, a specificity of 92.6%, and an AUC of 97.7% were obtained for the diagnosis of MPE.[25] In the study, various clinical characteristics of the patients were not addressed, and the sample size was small; previous reports have also indicated that the results may differ if these limitations are mitigated.

Ultrasonography (USG) is widely used for diagnosing and monitoring lung pathologies due to its safety, bedside applicability, and low cost, though its main limitation is operator dependence. In a study aiming to develop an automated PE diagnosis system, a dataset of 623 videos comprising 99,209 two dimensional (2D) USG images from 70 patients was created.[26] Two models were trained using frame- and video-based labels. Based on expert interpretations, the models achieved accuracies of 92.4% and 91.1%, respectively, with no significant difference between them. The study demonstrated that PE can be reliably and efficiently diagnosed from USG images using AI. In another study, a DL model was developed for accurate segmentation of lung USG images of PE, and its performance was compared with that of experts.[27] A total of 3,041 USG images from 24 PE patients were segmented by two USG experts and used as the ground truth. The model's performance, assessed by DSC, was 0.70 for comparisons between the AI and experts, while the expert-to-expert DSC was 0.61. These results indicate that the algorithm's accuracy is comparable to that of human experts, supporting its potential as a reliable tool in PE diagnosis and management.

Artificial Intelligence in the Diagnosis of Tuberculous Pleurisy

TP is one of the most common forms of extrapulmonary tuberculosis (TB).[28,29] The incidence of TP varies according to the prevalence of TB. While it constitutes 4% of all TB cases in the USA, TP constitutes 20% of cases in South Africa.[29] The gold standard for the diagnosis of TP is the demonstration of TB bacilli in PE or biopsy samples. Elevated ADA and interferon-gamma (IFN-γ) levels in PE are important supportive diagnostic markers.[30,31] Comprehensive PE analysis, including ADA and IFN-γ levels, yields higher diagnostic accuracy; however, different cut-off values are reported.[30-32] On the other hand, the efficiency of these markers varies with disease prevalence and age group.[30,31] The microbiological culture positivity of PE for the diagnosis of TP ranges from 12% to 70%, and the highest reported diagnostic yield is 30%.[30] When solid media are used, it can take up to 8 weeks to obtain the results.[30] Pleural biopsy is another invasive, costly, and complication-prone diagnostic procedure. TP usually heals spontaneously, but 43-65% of these patients develop TB within a few years.[30,31] Therefore, early diagnosis and treatment of TP are important to prevent both fibrothorax and recurrent TB disease. It is necessary to develop a less-invasive, low-cost method with a high diagnostic yield for the diagnosis of TP.[28,30-32]

Several studies have explored the potential of AI models to enhance clinicians' diagnostic performance in TP. Ren et al.[32] compared the performance of four AI models—LR, k-nearest neighbour (KNN), SVM, and RF—against pleural fluid adenosine deaminase (pfADA) levels using a dataset of 443 PE cases that included demographic, clinical, and fluid analysis data. Combining AI models with pfADA yielded the highest diagnostic performance: 85.4% sensitivity, 84.1% specificity, and 84.7% accuracy at a pfADA cut-off of 17.5 U/L. When the cut-off is set at 17.5 U/L, the threshold can support clinical decision-making by favoring early initiation of anti-TB treatment in patients with a high pretest probability and concordant imaging or clinical findings, while deferring invasive procedures such as pleural biopsy. LR estimates outcome probabilities; KNN classifies based on the majority class of nearby samples; SVM identifies a hyperplane maximizing class separation; and RF uses multiple decision trees, combining their outputs to reduce overfitting and improve stability. Among all models, RF achieved the best performance (AUC: 0.971; sensitivity: 89.1%; specificity: 93.6%; PPV: 91.3%; NPV: 91.5%), outperforming LR (AUC: 0.876), KNN (AUC: 0.895), and SVM (AUC: 0.918), and pfADA alone.

A prospective multicentre study assessed, using ML, the diagnostic value of ADA levels, routine pleural fluid parameters (pH, glucose, protein, LDH, cell counts), and age for TP diagnosis in low-prevalence areas.[33] The SVM model showed the best performance with 97% accuracy, AUC: 0.98, 91% sensitivity, and 98% specificity. When ADA >40 U/L and lymphocyte ratio >50% were used, sensitivity and specificity were 97% and 93%, respectively, with a 100% NPV. In low-prevalence settings, this high NPV can help avoid unnecessary invasive diagnostic procedures by reliably ruling out TP. Including age and routine clinical parameters increased ADA specificity to 98% and PPD positivity rate to 64%, supporting its non-invasive diagnostic value. Another study used a decision tree and a weighted sparse representation-based classification (WSRC) model to differentiate TP from MPE based on pleural biomarkers.[34] Among 236 patients, ADA had the best individual performance (sensitivity: 91.9; specificity: 74%). Accuracy improved when age, polynuclear leukocytes, and lymphocytes were added. WSRC achieved an AUC of 0.877, sensitivity 93.3%, specificity 82.0%, PPV 87.5%, and NPV 90.1%. A decision flowchart based on these markers achieved an accuracy of 88.8% and provided a cost-effective and reliable tool. Liu et al.[35] developed several ML models for early TP diagnosis using data from 1,435 patients (plus 153 for external validation). The SVM model performed best, with 87.7% accuracy, 85.3% precision, an AUC of 0.914, 94.7% sensitivity, and 80.7% specificity. PE-ADA, PE-CEA, and serum CYFRA21-1 were the top predictors. In another study, five AI models—including LR, RF, gradient boosting, deep neural networks, and a contrastive-loss model—were compared to assess the etiology of PE, with ADA levels incorporated.[36] The contrastive-loss model had the best performance (sensitivity: 84.1%; specificity: 94.1%), surpassing those of traditional ADA-based criteria (sensitivity: 80.2%; specificity: 90.3%).

Li et al.[37] aimed to develop a novel AI model to diagnose TP. The study used 77 features, including clinical symptoms, routine blood tests, biochemical markers, pleural fluid cell counts, and fluid biochemistry. To optimize performance and identify key diagnostic factors, a FS model was used. The top five features were PE-ADA level, percentage of lymphocytes in pleural effusion (PELP), age, body temperature, and pleural fluid

color. An SVM model classified patients as TP or non-TP. The moth flame optimization (MFO) algorithm optimized the SVM parameters to achieve optimal performance. The resulting FS-MFO-SVM model achieved 95% accuracy, 93.35% sensitivity, 97.57% specificity, and an AUC of 95.6. This model predicts TP using patient data, such as clinical signs, blood tests, and pleural fluid analysis, with decisions primarily based on PE-ADA, PELP, age, temperature, and fluid color. The authors suggested that this non-invasive method could be an alternative to pleural biopsy and could hold promise for use in resource-limited settings due to its low cost and portability.

Artificial Intelligence in the Diagnosis of Pneumothorax

Pneumothorax can cause significant morbidity and mortality depending on the severity of the air leak and on the patient's cardiopulmonary reserve, as it impairs oxygenation and ventilation. Rapid detection and intervention are therefore essential. Chest radiography is the first-line and most commonly used imaging modality for diagnosis. However, pneumothorax may go undetected in 20% of cases, requiring thoracic CT. Researchers have evaluated the performance of radiologists and AI using large CXR datasets, with promising results. AI can be particularly helpful in settings that lack experienced clinicians or radiologists, both for detection and for severity grading. However, digital image quality and the presence of chest tubes have been shown to limit AI performance. On CXRs, AI models may misidentify a chest tube as a pneumothorax or focus on the tube instead of the actual air leak, reducing diagnostic accuracy.[6,38]

Various AI models have been developed for pneumothorax detection, and many of these models have received Food and Drug Administration (FDA) approval. The sensitivity of FDA-approved AI tools for diagnosing pneumothorax ranges from 84.3% to 94.6%, and specificity ranges from 87.9% to 95.1%. AI can be used primarily for triage and to provide a second opinion. AI requires less time to read radiographs than physicians do. Pneumothorax among patients presenting to the emergency department is very rare, when considering all radiographs obtained. An AI-enabled pneumothorax detection tool can rapidly identify true-positive cases and reduce waiting times for these cases in the emergency department.[39,40]

Studies comparing the performance of AI with that of radiologists are crucial for understanding AI's effectiveness and limitations in medical imaging. In a meta-analysis of 63 studies, the overall AUC was found to be 0.97 for both AI and physicians.[39] In this meta-analysis, the average sensitivity was 84% for AI and 85% for physicians; the average specificity was 96% for AI and 98% for physicians. In a multicenter retrospective study of 2,040 patients, Plesner et al.[41] reported that AI models detected pneumothorax with sensitivities of 63-90% and specificities of 98-100%. False-negative rates were comparable to those in radiology reports, but AI showed higher false-positive rates. Sensitivity decreased for small lesions, and specificity was lower for A-P chest radiographs and cases with multiple simultaneous pathologies. Kim et al.[42] developed an AI-based model to calculate pneumothorax area and compared its performance with that of an experienced radiologist and a gold-standard CT-based method. The measured pneumothorax rates were 5.41% for the radiologist and 8.45% for AI, representing a 3.04 percentage-point gap favoring the radiologist. However, no significant difference was observed between AI predictions and the gold standard ($P = 0.11$). The AI model successfully predicted the need for thoracostomy when the proportion of the chest radiograph occupied by pneumothorax exceeded 21.6%. Despite limitations such as a retrospective design and small sample size, the study highlights AI's potential utility in clinical practice. A study of 500 chest radiographs that investigated radiologists' performance with and without AI assistance found that unaided radiologists achieved the highest sensitivity (75.7%) and specificity (99-99.7%) in the diagnosis of pneumothorax.[43] AI alone achieved 99% specificity for pneumothorax and improved sensitivity for all findings compared with unaided readers. Additionally, AI assistance reduced average reading times by 25 seconds (from 81 to 56 seconds, $P < 0.001$) without affecting specificity. However, AI-assisted radiologists did not outperform AI alone, possibly because mistrust of AI led to accurate detections being dismissed. The study highlights AI's potential to enhance diagnostic sensitivity and efficiency across expertise levels while reducing reading times for chest radiographs.

Hillis et al.[40] evaluated the performance of an AI model designed to detect pneumothorax and tension pneumothorax. This AI model identified pneumothorax with 94.3% sensitivity, 92.0% specificity, and an AUC of 0.979, and detected tension pneumothorax with 94.5% sensitivity, 95.3% specificity, and an AUC of 0.987. When subgroup analyses were conducted for gender, age, patient's position, and projections, all subgroups achieved at least a sensitivity of 80%, and a specificity of 80% with an AUC of 0.95. Even in the presence or absence of potentially biasing findings, detection of both pneumothorax and tension pneumothorax maintained 80% sensitivity and 80% specificity, with an AUC of 0.95.

Thian et al.[44] investigated the performance and generalizability of an AI model on 2,931 chest radiographs. The mean AUC was 0.94, with a sensitivity of 88%, specificity of 88%, PPV of 71%, and NPV of 95%. The model demonstrated lower performance for small pneumothoraces compared to larger ones (AUC 0.88 vs. 0.96; $P = 0.005$). The model's performance did not differ between radiographs with and without chest tubes (AUC 0.95 vs. AUC 0.94; $P > 0.99$) or between radiographic projections (A-P vs. P-A; AUC 0.92 vs. AUC 0.96; $P = 0.05$). Thian et al.[44] showed that the AI model trained on a large database became generalizable after limiting factors unrelated to the training data were eliminated. In the study by Lee et al.[45], the overall PPV for AI-assisted pneumothorax diagnosis was reported to be 41.1%. The PPV was higher for P-A views (88.2%), but dropped to 20.1% for A-P views. Younger age, P-A projection, and larger pneumothorax were associated with increased PPV for AI-assisted pneumothorax diagnosis. In 31.3% of false-positive cases flagged by AI, the underlying cause was identified: 20.5% were due to skin folds, 5.6% to chest wall abnormalities, 3.1% to bullae, and 2.1% to rib opacities.

Hong et al.[46] evaluated 1,319 patients who underwent transthoracic lung biopsy, using an AI model to assess post-procedural chest radiographs for iatrogenic pneumothorax.

They found that the AI-assessed group had higher sensitivity (85.4% vs. 67.1%), NPV (96.8% vs. 91.3%), and accuracy (96.8% vs. 92.3%) than radiologists' interpretations ($P < 0.001$).[46] There were no significant differences between the groups in specificity and PPV ($P = 0.46$ and $P = 0.45$). In analyses based on pneumothorax volume, the AI model showed higher sensitivity in patients with pneumothorax <10% (74.5% vs. 51.4%, $P = 0.009$) and in those with pneumothorax 10-15% (92.7% vs. 70.2%, $P = 0.008$). Among patients with pneumothorax, the AI-assessed group required fewer catheters than the other group (2.4% vs. 5%, $P = 0.009$). At the conclusion of the study, the researchers suggested that the AI model could be used to diagnose iatrogenic pneumothorax on CXRs, allowing patients with small pneumothoraces to be diagnosed earlier and treated conservatively before air leakage progresses.

Artificial Intelligence in the Diagnosis of Malignant Pleural Mesothelioma

MPM is associated with asbestos exposure in 80% of cases. Although asbestos is banned in many countries, MPM incidence continues to rise. Given a poor prognosis and average survival of 9-14 months after diagnosis, rapid and accurate detection and assessment of treatment response are essential. Prognosis and treatment monitoring often rely on tumor segmentation in serial thoracic CT scans and interpretation of PET-CT images-processes prone to human error and a high workload for radiologists. 3D CT image analysis offers advantages for more accurate prognosis and treatment evaluation. Accordingly, various AI models have been developed and investigated for MPM applications.[47-50]

Segmentation of MPM is highly challenging, as it relies solely on density differences to distinguish tumor tissue from surrounding benign soft tissue. In Sensakovic et al.[47] study, a system was developed to automate segmentation and volumetric measurement. This method yielded 3D positional and volumetric information that was validated against 2D manual detections, significantly reducing human error and saving time. This allowed pleural abnormalities to be objectively monitored through serial imaging and for changes in size to be detected. In a study by Karapınar Şentürk and Çekiç[48], the performance of five AI models for diagnosing MPM was evaluated in terms of accuracy and sensitivity. The models' accuracies ranged from 80% to 100%, and sensitivities ranged from 50% to 100%. SVM and Artificial Neural Networks (ANN) demonstrated the highest accuracy and sensitivity (100%). However, because the majority of samples in this study belonged to non-diseased groups, these rates may differ in real-world settings. Another study investigated the performance of a 3D DCNN-based AI model that used PET-CT to differentiate MPM from benign pleural diseases.[49] Results from four datasets were analyzed: PET-CT-AI; radiologist interpretation; maximum standardized uptake value (SUV_{max}) quantitative method; and PET-CT combined with SUV_{max}, gender, and age, with AI. The AUC values were 82.5%, 85.4%, 88.1%, and 89.6. In the last protocol, sensitivity, specificity, and accuracy were 88.5%, 73.6%, and 82.4%, respectively. AI integrated solely with PET-CT demonstrated inferior performance compared with expert interpretation and SUV_{max}-based quantitative methods. However, AI integrating PET-CT, SUV_{max}, gender, and age demonstrated superior diagnostic performance compared with human interpretation and SUV_{max}-based methods. In a study by Er and Tanrikulu[50] involving 324 MPM cases, a newly developed AI system achieved an accuracy rate of 97.7%, outperforming the ANN algorithm. This algorithm has been reported to be an excellent auxiliary tool for diagnosing MPM.

No single PE biomarker provides sufficient diagnostic accuracy for MPM. Therefore, using multiple biomarkers could be a suitable approach to improve diagnostic efficiency. The integration of multiple biomarkers using AI models can enhance diagnostic yield. In a study involving 188 patients with undiagnosed PE, six ML-based AI models were tested using the biomarkers SMRP, CEA, and CYFRA21-1: LR, linear discriminant analysis, multivariate adaptive regression splines, KNN, GBM, and RF.[51] Among these algorithms, the LR model significantly improved the diagnostic accuracy for MPM, achieving an AUC of 0.97 and an accuracy of 91%. Similarly, another study examined four AI models for the differential diagnosis of MPM based on cytological analysis and tumor marker concentrations.[52] The logic learning machine (LLM) showed the highest performance, with an accuracy of 77.5%, while the accuracies of the other three methods —KNN, ANN, and decision tree models— ranged from 54.4% to 72.8%. Furthermore, the LLM achieved diagnostic accuracies of 79% for MPM, 66% for pleural metastasis, and 89% for benign pleural diseases.

DISCUSSION

Most of the current AI studies in pleural diseases are based on relatively small, single-center cohorts, which inherently limit their external validity and generalizability. While reported accuracy and AUC values are often high, these findings should be interpreted with caution, as the real-world performance of AI models may differ substantially in heterogeneous patient populations and across diverse clinical settings. Therefore, large-scale, multicenter validation studies are urgently needed to confirm their clinical applicability.

Strengths and Limitations of Artificial Intelligence in Pleural Diseases

Despite promising results, AI models in pleural diseases face several important limitations (Table 2). Data imbalance and selection bias may lead to overfitting, reducing the reliability of predictions when applied to broader populations. Another critical issue is explainability: the so-called "black-box" nature of DL algorithms limits clinicians' ability to understand how specific outputs are generated, thereby reducing clinicians' trust in the technology. Furthermore, the lack of transparency complicates clinical decision-making, especially in high-stakes scenarios such as invasive interventions. Finally, the majority of existing models are validated retrospectively, which underscores the need for prospective, multicenter studies with rigorous external validation before routine clinical adoption.

Implementation and Clinical Integration

For the rational integration of AI into pleural disease

Table 2. Strengths and limitations of artificial intelligence models in pleural diseases

Modality/AI application	Strengths	Limitations	References
Chest X-ray	Widely available, fast triage (PE, pneumothorax); FDA-cleared tools exist; high sensitivity/specificity in large datasets	Lower accuracy in small effusions/pneumothorax; susceptible to artifacts (skin folds, tubes); generalizability depends on dataset diversity	9-11,38-46
Chest CT	Excellent anatomical detail; robust segmentation with nnU-Net; reproducible volume analysis; useful for simple vs. complex PE classification	Consistently underestimates absolute fluid volume; requires calibration; high radiation exposure; most studies single-center with limited validation	12,13,17-19
PET-CT	Adds functional data for MPE vs. BPE and MPM prognosis; multimodal fusion improves performance; high reported AUC	Small sample sizes; expensive and limited availability; performance may drop in real-world heterogeneous populations	16,25,49
Cytology/WSI	AI systems (e.g., Aitrox) achieve performance comparable to expert cytopathologists; potential to reduce inter-observer variability; supports rapid triage	Dependent on quality of slide preparation; limited datasets; still requires pathologist oversight; "black box" decisions reduce trust	23,24
Lung ultrasound	Safe, bedside, radiation-free; AI reduces operator dependency; early studies show >90% accuracy	Limited training data: performance varies with probe settings and acquisition quality; segmentation less robust than CT	26,27
Tuberculous pleurisy models	AI + ADA and lab parameters improve diagnostic yield; potential non-invasive alternative to biopsy in resource-limited settings	Cut-off values differ by geography/epidemiology; small sample sizes; external validation rare	32-37
Malignant pleural mesothelioma	AI-based segmentation improves reproducibility in tumor volume monitoring; multimodal models integrate PET-CT + biomarkers with promising accuracy	Challenging tumor-benign tissue differentiation; many studies use retrospective datasets; real-world validation lacking	47-52

AI: artificial intelligence, CT: computed tomography, PET: positron emission tomography, WSI: whole-slide imaging, PE: pleural effusion, FDA: Food and Drug Administration, nnU-Net: no-new-U-Net segmentation framework, MPE: malignant pleural effusion, BPE: benign pleural effusion, MPM: malignant pleural mesothelioma, AUC: area under the curve, ADA: adenosine deaminase

management, stepwise frameworks should be considered. At the initial stage, AI can serve as a triage and screening tool, for example in chest radiography for effusion or pneumothorax detection. At the intermediate level, AI models may provide decision support by predicting the likelihood of malignancy and guiding the necessity of invasive procedures such as thoracentesis or biopsy. At the advanced level, AI may assist in treatment monitoring, such as evaluating changes in effusion volume or tumor burden in MPM. Importantly, AI should be viewed as an adjunctive decision-support system rather than a replacement for physician judgment, with outputs always interpreted within the broader clinical context. Our findings are consistent with the recent narrative review by Marchi et al.,[7] which also emphasized the importance of critically evaluating AI models, particularly regarding their generalizability and the necessity of developing frameworks for rational integration into clinical workflows.

AI applications for pleural diseases require careful planning for translation into clinical workflows. Intended clinical roles include triage and second-read tools for pneumothorax on chest radiographs, automated segmentation and volume tracking of PEs on CT, and cytology triage systems to prioritize suspicious samples for pathologist review.

• Integration: Seamless interoperability with Picture Archiving and Communication Systems and Electronic Health Records is essential. AI outputs should be provided in DICOM-compatible formats, incorporated into structured reports, and logged with audit trails to maintain accountability.

• Regulatory examples: The approval and deployment of FDA-cleared pneumothorax detection algorithms provide precedents for the integration of AI in pleural disease workflows. These experiences highlight the importance of prospective validation, calibration, and clinician oversight in safe implementation.

• Training: Adoption requires short, role-specific training sessions for radiologists, pulmonologists, and pathologists. Training should cover interpretation of confidence scores, handling of false positives, and recognition of model limitations.

• Cost and time-saving considerations: Evidence from real-world radiology practice suggests that AI triage can reduce report turnaround times and improve sensitivity. Automated CT segmentation and cytology triage also have the potential to reduce workload and shorten diagnostic delays. Formal cost-effectiveness analyses remain necessary to confirm the economic value of these tools in pleural disease management.

Future Directions

To accelerate translation of AI in pleural diseases into clinical practice, the following priorities are needed:

• Multicentre prospective trials with predefined thresholds and patient-relevant outcomes to validate diagnostic performance in real-world settings.

• Domain-shift and out-of-distribution testing across different scanners, institutions, and patient populations to ensure generalizability.

• Multimodal data fusion combining imaging (CT, PET-CT, USG), cytology, and clinical data to enhance predictive accuracy and robustness.

• Real-time USG guidance tools to support novice operators and improve procedure safety and efficiency.

• Economic evaluations and cost-effectiveness analyses to clarify resource savings and sustainability within healthcare systems.

• Bias and calibration checks at deployment sites, with continuous monitoring dashboards to maintain safety and fairness.

• Creation of open datasets and benchmarks for pleural imaging, cytology, and biomarker AI tasks to foster reproducibility and global collaboration.

• These steps will provide the field with a clear roadmap, bridging experimental success toward responsible clinical implementation.

CONCLUSION

Based on current evidence, the most promising AI applications in pleural diseases are listed in Table 3. These include radiological segmentation models for PE quantification, DL algorithms to differentiate malignant from benign effusions using CT and PET-CT, and ML-based classification systems utilizing pleural fluid biomarkers. Among these, ensemble models like XGBoost, RF, and SVM that combine clinical, radiological, and laboratory data have demonstrated high diagnostic accuracy—particularly in distinguishing MPE from TP, often with AUCs above 0.90. Automated segmentation tools such as nnU-Net and contrastive learning models have shown near-expert accuracy and consistency in volume and lesion analysis. Additionally, computer-aided cytological tools like Aitrox and CAD systems for MPE detection have matched the diagnostic performance of experienced cytopathologists, suggesting potential for workflow standardization. Altogether, these AI innovations offer non-invasive, rapid, and objective clinical support and may redefine diagnostic approaches in pleural disease management.

Although AI applications hold great promise for the future, their integration into routine clinical practice still faces several challenges. First, the algorithms require further optimization and performance improvement. Most current studies are based on single-center, small-scale datasets, lacking standardized performance metrics and limiting generalizability. To enable routine use, large-scale, multicenter studies with standardized protocols are essential, along with strong collaboration among patients, clinicians, institutions, and medical technology companies.

Table 3. Top performing artificial intelligence applications in pleural diseases

Application area	Model/algorithm	Key performance metrics	Readiness	References
PE diagnosis (CXR)	Deep learning	AUC: 97% Sensitivity: 95% Specificity: 97%	Research	[9]
PE volume measurement (CT)	nnU-Net segmentation model	DSC: 0.89 ICC ≥0.995	Research	[12,13]
Pneumothorax detection (CXR)	FDA-approved AI systems	Sensitivity: 84-94%, specificity: 88-95%	FDA-cleared	[39,40]
MPE-BPE differentiation (CT)	XGBoost + clinical variables	AUC >0.90 Sensitivity >85%	Research	[16]
Cytological MPE diagnosis	Aitrox (DCNN, WSI)	AUC: 0.95 Accuracy: 91.7%, specificity: 94.4%	Research	[24]
MPM diagnosis (PET-CT + markers)	LLM, LR, 3D DCNN	AUC: 0.89-0.97 Accuracy: 82-91%	Research	[49,51]

PE: pleural effusion, CXR: chest X-ray, CT: computed tomography, MPE: malignant pleural effusion, BPE: benign pleural effusion, MPM: malignant pleural mesothelioma, PET: positron emission tomography, nnU-Net: no-new-U-Net segmentation framework, FDA: Food and Drug Administration, DCNN: deep convolutional neural network, WSI: whole-slide imaging, LLM: logic learning machine, LR: logistic regression, AUC: area under the curve, DSC: dice similarity coefficient, ICC: intraclass correlation coefficient, 3D: three dimensional

Footnotes

Authorship Contributions

Surgical and Medical Practices: F.K., Ö.D., Concept: F.K., Ö.D., Design: F.K., Ö.D., Data Collection or Processing: F.K., Analysis or Interpretation: F.K., Literature Search: F.K., Writing: F.K., Ö.D.

Conflict of Interest: No conflict of interest was declared by the authors.

Financial Disclosure: The authors declared that this study received no financial support.

REFERENCES

1. Mummadi SR, Stoller JK, Lopez R, Kailasam K, Gillespie CT, Hahn PY. Epidemiology of adult pleural disease in the United States. *Chest: Elsevier Inc.* 2021:1534-1551. **[Crossref]**
2. Sundaralingam A, Bedawi EO, Rahman NM. Diagnostics in pleural disease. *Diagnostics (Basel).* 2020;10(12):1046. **[Crossref]**
3. Addala DN, Rahman NM. Man versus machine in pleural diagnostics: does artificial intelligence provide the solution? *Ann Am Thorac Soc.* 2024;21(2):202-203. **[Crossref]**
4. Feller-Kopman D, Light R. Pleural disease. *N Engl J Med.* 2018;378(8):740-751. **[Crossref]**
5. Zhang C, Wu W, Yang J, Sun J. Application of artificial intelligence in respiratory medicine. *J Digit Health.* 2022;1(1):30-39. **[Crossref]**
6. Kalaiyarasan K, Sridhar R. Artificial intelligence in respiratory medicine: the journey so far - a review. *J Assoc Pulmonologist Tamil Nadu.* 2023;6(2):53-68. **[Crossref]**
7. Marchi G, Mercier M, Cefalo J, et al. Advanced imaging techniques and artificial intelligence in pleural diseases: a narrative review. *Eur Respir Rev.* 2025;34(176):240263. **[Crossref]**
8. Li D, Pehrson LM, Lauridsen CA, et al. The added effect of artificial intelligence on physicians' performance in detecting thoracic pathologies on CT and chest X-ray: a systematic review. *Diagnostics (Basel).* 2021;11(12):2206. **[Crossref]**
9. Chang J, Lin BR, Wang TH, Chen CM. Deep learning model for pleural effusion detection via active learning and pseudo-labeling: a multisite study. *BMC Med Imaging.* 2024;24(1):92. **[Crossref]**
10. Huang T, Yang R, Shen L, et al. Deep transfer learning to quantify pleural effusion severity in chest X-rays. *BMC Med Imaging.* 2022;22(1):100. **[Crossref]**
11. Zhou L, Yin X, Zhang T, et al. Detection and semiquantitative analysis of cardiomegaly, pneumothorax, and pleural effusion on chest radiographs. *Radiol Artif Intell.* 2021;3(4):e200172. **[Crossref]**
12. Sexauer R, Yang S, Weikert T, et al. Automated detection, segmentation, and classification of pleural effusion from computed tomography scans using machine learning. *Invest Radiol.* 2022;57(8):552-559. **[Crossref]**
13. Hwang EJ, Hong H, Ko S, et al. Accuracy of fully automated and human-assisted artificial intelligence-based CT quantification of pleural effusion changes after thoracentesis. *Radiol Artif Intell.* 2025;7(1):e240215. **[Crossref]**
14. Feller-Kopman DJ, Reddy CB, Gould MK, et al. Management of malignant pleural effusions: an official ATS/STS/STR clinical practice guideline. *Am J Respir Crit Care Med.* 2018;198(7):839-849. **[Crossref]**
15. Reddy CB, DeCamp MM, Diekemper RL, et al. Summary for clinicians: clinical practice guideline for management of malignant pleural effusions. *Ann Am Thorac Soc.* 2019;16(1):17-21. **[Crossref]**
16. Wang S, Tan X, Li P, et al. Differentiation of malignant from benign pleural effusions based on artificial intelligence. *Thorax.* 2023;78(4):376-382. **[Crossref]**
17. Ozcelik N, Ozcelik AE, Guner Zirih NM, Selimoglu I, Gumus A. Deep learning for diagnosis of malign pleural effusion on computed tomography images. *Clinics (Sao Paulo).* 2023;78:100210. **[Crossref]**
18. Li Y, Tian S, Huang Y, Dong W. Driverless artificial intelligence framework for the identification of malignant pleural effusion. *Transl Oncol.* 2021;14(1):100896. **[Crossref]**
19. Kim NY, Jang B, Gu KM, Park YS, Kim YG, Cho J. Differential diagnosis of pleural effusion using machine learning. *Ann Am Thorac Soc.* 2024;21(2):211-217. **[Crossref]**
20. Zhang Y, Wang J, Liang B, Wu H, Chen Y. Diagnosis of malignant pleural effusion with combinations of multiple tumor markers: a comparison study of five machine learning models. *Int J Biol Markers.* 2023;38(2):139-146. **[Crossref]**
21. Wei TT, Zhang JF, Cheng Z, Jiang L, Li JY, Zhou L. Development and validation of a machine learning model for differential diagnosis of malignant pleural effusion using routine laboratory data. *Ther Adv Respir Dis.* 2023;17:17534666231208632. **[Crossref]**
22. Loveland P, Christie M, Hammerschlag G, Irving L, Steinfort D. Diagnostic yield of pleural fluid cytology in malignant effusions: an Australian tertiary centre experience. *Intern Med J.* 2018;48(11):1318-1324. **[Crossref]**
23. Win KY, Choomchuay S, Hamamoto K, Raveesunthornkiat M, Rangsirattanakul L, Pongsawat S. Computer aided diagnosis system for detection of cancer cells on cytological pleural effusion images. *Biomed Res Int.* 2018;2018:6456724. **[Crossref]**
24. Xie X, Fu CC, Lv L, et al. Deep convolutional neural network-based classification of cancer cells on cytological pleural effusion images. *Mod Pathol.* 2022;35(5):609-614. **[Crossref]**
25. Wei J, Li P, Zhang H, Zhu R. Clone selection artificial intelligence algorithm-based positron emission tomography-computed tomography image information data analysis for the qualitative diagnosis of serous cavity effusion in patients with malignant tumors. *J Healthc Eng.* 2021;2021:4272411. **[Crossref]**
26. Tsai CH, van der Burgt J, Vukovic D, et al. Automatic deep learning-based pleural effusion classification in lung ultrasound images for respiratory pathology diagnosis. *Phys Med.* 2021;83:38-45. **[Crossref]**
27. Vukovic D, Wang A, Antico M, et al. Automatic deep learning-based pleural effusion segmentation in lung ultrasound images. *BMC Med Inform Decis Mak.* 2023;23(1):274. **[Crossref]**
28. Chan KKP, Lee YCG. Tuberculous pleuritis: clinical presentations and diagnostic challenges. *Curr Opin Pulm Med.* 2024;30(3):210-216. **[Crossref]**
29. Global Tuberculosis Report 2024. Accessed September 7, 2025. **[Crossref]**
30. Jeon D. Tuberculous pleurisy: an update. *Tuberc Respir Dis (Seoul).* 2014;76(4):153-159. **[Crossref]**
31. Shaw JA, Diacon AH, Koegelenberg CFN. Tuberculous pleural effusion. *Respirology.* 2019;24(10):962-971. **[Crossref]**
32. Ren Z, Hu Y, Xu L. Identifying tuberculous pleural effusion using artificial intelligence machine learning algorithms. *Respir Res.* 2019;20(1):220. **[Crossref]**
33. Garcia-Zamalloa A, Vicente D, Arnay R, et al. Diagnostic accuracy of adenosine deaminase for pleural tuberculosis in a low prevalence setting: a machine learning approach within a 7-year prospective multi-center study. *PLoS One.* 2021;16(11):0259203. **[Crossref]**

34. Darooei R, Sanadgol G, Gh-Nataj A, et al. Discriminating tuberculous pleural effusion from malignant pleural effusion based on routine pleural fluid biomarkers, using mathematical methods. *Tanaffos*. 2017;16(2):157-165. **[Crossref]**
35. Liu Y, Liang Z, Yang J, et al. Diagnostic and comparative performance for the prediction of tuberculous pleural effusion using machine learning algorithms. *Int J Med Inform*. 2024;182:105320. **[Crossref]**
36. Lee JH, Choi CM, Park N, Park HJ. Classification of pleural effusions using deep learning visual models: contrastive-loss. *Sci Rep*. 2022;12(1):5532. **[Crossref]**
37. Li C, Hou L, Sharma BY, et al. Developing a new intelligent system for the diagnosis of tuberculous pleural effusion. *Comput Methods Programs Biomed*. 2018;153:211-225. **[Crossref]**
38. Irmici G, Cè M, Caloro E, et al. Chest X-ray in emergency radiology: what artificial intelligence applications are available? *Diagnostics (Basel)*. 2023;13(2):216. **[Crossref]**
39. Sugibayashi T, Walston SL, Matsumoto T, Mitsuyama Y, Miki Y, Ueda D. Deep learning for pneumothorax diagnosis: a systematic review and meta-analysis. *Eur Respir Rev*. 2023;32(168):220259. **[Crossref]**
40. Hillis JM, Bizzo BC, Mercaldo S, et al. Evaluation of an artificial intelligence model for detection of pneumothorax and tension pneumothorax in chest radiographs. *JAMA Netw Open*. 2022;5(12):e2247172. **[Crossref]**
41. Plesner LL, Müller FC, Brejnebøl MW, et al. Commercially available chest radiograph AI tools for detecting airspace disease, pneumothorax, and pleural effusion. *Radiology*. 2023;308(3):e231236. **[Crossref]**
42. Kim D, Lee JH, Kim SW, et al. Quantitative measurement of pneumothorax using artificial intelligence management model and clinical application. *Diagnostics (Basel)*. 2022;12(8):1823. **[Crossref]**
43. Bennani S, Regnard NE, Ventre J, et al. Using AI to improve radiologist performance in detection of abnormalities on chest radiographs. *Radiology*. 2023;309(3):e230860. **[Crossref]**
44. Thian YL, Ng D, Hallinan JTPD, et al. Deep learning systems for pneumothorax detection on chest radiographs: a multicenter external validation study. *Radiol Artif Intell*. 2021;3(4):e200190. **[Crossref]**
45. Lee S, Kim EK, Han K, Ryu L, Lee EH, Shin HJ. Factors for increasing positive predictive value of pneumothorax detection on chest radiographs using artificial intelligence. *Sci Rep*. 2024;14(1):19624. **[Crossref]**
46. Hong W, Hwang EJ, Lee JH, Park J, Goo JM, Park CM. Deep learning for detecting pneumothorax on chest radiographs after needle biopsy: clinical implementation. *Radiology*. 2022;303(2):433-441. **[Crossref]**
47. Sensakovic WF, Armato SG 3rd, Straus C, et al. Computerized segmentation and measurement of malignant pleural mesothelioma. *Med Phys*. 2011;38(1):238-244. **[Crossref]**
48. Karapınar Şentürk Z, Çekiç N. A machine learning based early diagnosis system for mesothelioma disease. *Düzce University Journal of Science Technology*. 2020;8(2):1604-1611. **[Crossref]**
49. Kitajima K, Matsuo H, Kono A, et al. Deep learning with deep convolutional neural network using FDG-PET/CT for malignant pleural mesothelioma diagnosis. *Oncotarget*. 2021;12(12):1187-1196. **[Crossref]**
50. Er O, Tanrikulu AÇ. Use of artificial intelligence techniques for diagnosis of malignant pleural mesothelioma. *Dicle Med J*. 2015;42(1):5-11. **[Crossref]**
51. Niu Y, De Hu Z. Diagnostic accuracy of pleural effusion biomarkers for malignant pleural mesothelioma: a machine learning analysis. *J Lab Precis Med*. 2021;6:4. **[Crossref]**
52. Parodi S, Filiberti R, Marroni P, et al. Differential diagnosis of pleural mesothelioma using logic learning machine. *BMC Bioinformatics*. 2015;16(Suppl 9):3. **[Crossref]**